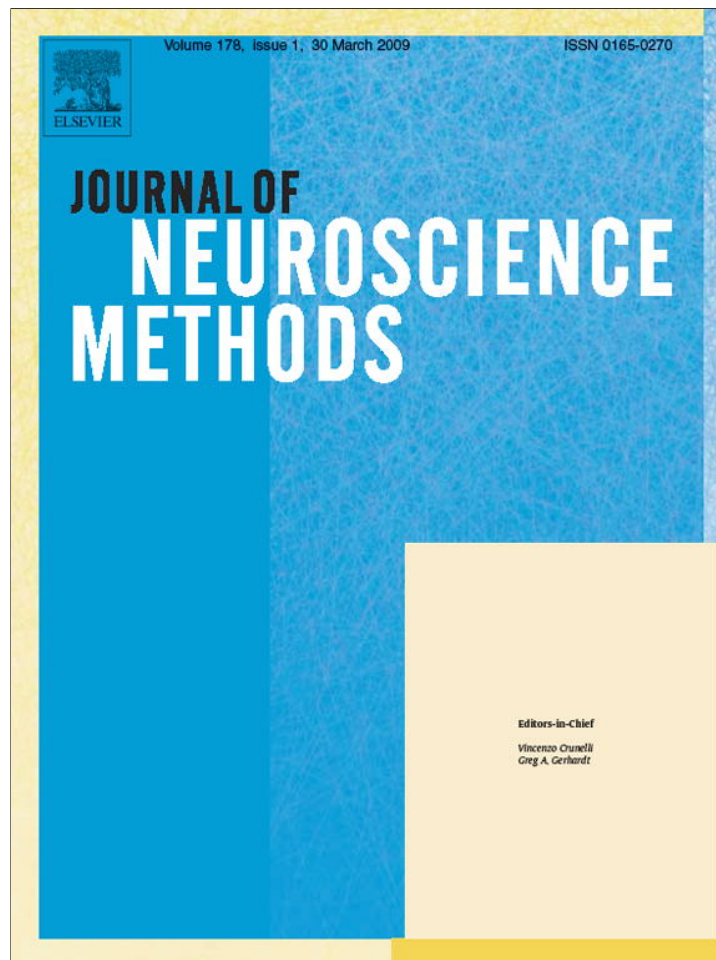


Provided for non-commercial research and education use.
Not for reproduction, distribution or commercial use.



This article appeared in a journal published by Elsevier. The attached copy is furnished to the author for internal non-commercial research and education use, including for instruction at the authors institution and sharing with colleagues.

Other uses, including reproduction and distribution, or selling or licensing copies, or posting to personal, institutional or third party websites are prohibited.

In most cases authors are permitted to post their version of the article (e.g. in Word or Tex form) to their personal website or institutional repository. Authors requiring further information regarding Elsevier's archiving and manuscript policies are encouraged to visit:

<http://www.elsevier.com/copyright>



Contents lists available at ScienceDirect

Journal of Neuroscience Methods

journal homepage: www.elsevier.com/locate/jneumeth

A multi-component decomposition algorithm for event-related potentials

Gang Yin^{a,b}, Jun Zhang^{b,*}, Yin Tian^a, DeZhong Yao^a^a Center of NeuroInformatics, School of Life Science and Technology, University of Electronic Science and Technology of China, ChengDu 610054, China^b Department of Psychology, The University of Michigan, 530 Church Street, Ann Arbor, MI 48109-1109, USA

ARTICLE INFO

Article history:

Received 29 April 2008

Received in revised form

16 November 2008

Accepted 17 November 2008

Keywords:

Event-related potentials

Stimulus component

Response component

Cue-component

Stimulus-lock

Response-lock

Reaction time

ABSTRACT

Event-related potentials (ERPs) are evoked activities of the brain related to specific events. They can be estimated by averaging across many trials aligned to a specific event onset time point, such as the stimulus, the response, or other behaviorally significant markers. If a single trial includes more than one such event (marker), as in all reaction-time tasks, the cross-contamination of components related to different events may mislead the explanation of ERPs. In order to recover event-related components, Zhang [Zhang J. Decomposing stimulus and response component waveforms in ERP. *Journal of Neuroscience Methods* 1998;80:49–63] provided a method for decomposing of ERPs according to two markers (stimulus and the behavioral response). Here we extend this formulation to deal with three or more markers in a single trial, and recover individual ERP components that are time-locked to those markers. As an application, we analyzed a cuing experiment with three events: cue, stimulus and response. The elapse between cue and stimulus was varied from trial to trial by the experimenter, and the time between stimulus and response was determined by the subjects (reaction-time variation). Our decomposition results show that the cue-dependent component waveform turns out to flatten out 500 ms after cue-onset, a finding consistent with our experimental paradigm.

© 2008 Elsevier B.V. All rights reserved.

1. Introduction

ERPs are evoked activities of the brain that are averaged over many trials to remove trial-by-trial noise and to increase signal-to-noise ratio. When the individual trials are aligned with respect to the stimulus onset, the ensemble average is called *stimulus-aligned* ERP, with waveforms demonstrating, e.g., P300 (Squires et al., 1975; Hillyard and Picton, 1987) and N400 (Kutas and Hillyard, 1980). When the ensemble averaging is performed by aligning individual trials to behavioral response onset, the so-called *response-aligned* ERP results, with waveforms demonstrating, e.g., error-related negativity (ERN) (Gehring et al., 1993; Falkenstein et al., 1995) or (after subtraction) lateralized readiness potential (LRP). In experimental paradigms where both a stimulus is presented and a behavioral response is required, stimulus-aligned ERP average and response-aligned ERP average may yield different waveforms since the subject does not respond with uniform reaction time across the ensemble of the trials. How to interpret these ensemble averages is thus a non-trivial problem, since either stimulus-aligned or response-aligned ERP average may contain both components related to the processing of stimulus (and hence better time-locked to the stimulus onset event) and com-

ponents related to the processing of response (and hence more tightly coupled with the moment of behavioral response onset). The overlapping event-related components in the ERP averaged waveform can cause difficulty and confusions in the interpretation of underlying neural mechanisms for ERP. For example, in the study of response inhibition by Go/Nogo paradigm, a question arises whether the N2/P3 differences between Go and Nogo trials in the overall ERP mainly comes from the accompanying motor response in the Go trial (Simson et al., 1977; Kok, 1986; Kopp et al., 1996). How to remove cross-contamination of ERP component waveforms in their ensemble averages was tackled and solved by Zhang (1998), who provided a method to uniquely recover a stimulus-locked component waveform and a response-locked component waveform from the stimulus-aligned ERP average and response-aligned ERP average (plus information about reaction time distribution that is behaviorally obtained).

Many psychological experiments involve more than two behavioral events in a single trial. For example, in the study of visual spatial attention where a peripheral or central cue is utilized, a single trial will involve three event-related components related to cue presentation, stimulus presentation and behavioral response, respectively. A similar situation occurs in the study of ERN when EMG measurement is introduced (Gehring and Fencsik, 1999)—in that case, the onset of EMG, along with the stimulus onset and response onset, constitute three independent behavioral events with variable separation between the onset times. This provides an

* Corresponding author. Tel.: +1 734 763 6161; fax: +1 734 763 7480.
E-mail address: junz@umich.edu (J. Zhang).

opportunity to understand underlying mechanisms of ERN, but also presents a challenge to unconfounding the ERP component waveforms time-locked to those events individually. So a more general formulation to decompose three or more components is needed to get different event-related components properly.

In this paper, the algorithm of ERP decomposition developed by Zhang (1998) is extended from the situation of two components (related to stimulus and response, respectively) to the situation of three or more events in a single trial. Though the general ideas follow those in Zhang (1998), implementation details are discussed in length. After having tested our new extended algorithm on simulated single-trial data, we applied it to separate ERP components in a Go/Nogo experiment with variable pre-cue, a paradigm involving three behavioral events in a trial.

2. Method

2.1. ERP decomposition for two components (S-R decomposition): a revisit to Zhang (1998)

Suppose we have the following experimental data: (a) the stimulus-aligned ERP average waveform denoted $F_s(t)$, (b) the response-aligned ERP average waveform $F_r(t)$, and (c) the distribution of reaction times $g(t)$. The problem is how to recover the stimulus-locked component (“S-component”) $f_s(t)$ and the response-locked component (“R-component”) $f_r(t)$. By reflecting on how $F_s(t)$, $F_r(t)$ are constructed and how $f_s(t)$, $f_r(t)$ are defined, the following two mathematical equations were derived (Zhang, 1998)

$$F_s(t) = f_s(t) + \int f_r(t - \tau)g(\tau) d\tau \quad (1)$$

$$F_r(t) = f_r(t) + \int f_s(t + \tau)g(\tau) d\tau \quad (2)$$

In convolution notation, they are

$$F_s(t) = f_s(t) + f_r(t) * g(t) \quad (3)$$

$$F_r(t) = f_r(t) + f_s(t) * g(-t) \quad (4)$$

Performing Fourier transform (those with tilde sign indicate the Fourier domain representation)

$$\tilde{F}_s(k) = \tilde{f}_s(k) + \tilde{f}_r(k) \cdot \tilde{g}(k) \quad (5)$$

$$\tilde{F}_r(k) = \tilde{f}_r(k) + \tilde{f}_s(k) \cdot \tilde{g}(-k) \quad (6)$$

and solving for the frequency components $\tilde{F}_s(k)$, $\tilde{F}_r(k)$, Zhang (1998) finally obtained

$$f_s(t) = \frac{1}{2\pi} \int \frac{\tilde{F}_s(k) - \tilde{F}_r(k) \cdot \tilde{g}(k)}{1 - |\tilde{g}(k)|^2} e^{ikt} dk \quad (7)$$

$$f_r(t) = \frac{1}{2\pi} \int \frac{\tilde{F}_r(k) - \tilde{F}_s(k) \cdot \tilde{g}(-k)}{1 - |\tilde{g}(k)|^2} e^{ikt} dk \quad (8)$$

where \sim represents the frequency spectrum of the recorded ERP averages and the RT distribution.

For convenience, we write out the above equations in matrix form. Here we adopt the periodic boundary condition (see Zhang,

1998). The Eqs. (3) and (4) in temporal domain can be cast as

$$\begin{bmatrix} F_s(1) \\ F_s(2) \\ \vdots \\ F_s(n) \\ F_r(1) \\ F_r(2) \\ \vdots \\ F_r(n) \end{bmatrix} = \begin{bmatrix} 1 & 0 & \dots & 0 & g(1) & g(2) & \dots & g(n) \\ 0 & 1 & \dots & \vdots & g(n) & g(1) & \dots & g(n-1) \\ \vdots & \vdots & \dots & \ddots & \vdots & \vdots & \dots & \vdots \\ 0 & \dots & 0 & 1 & g(2) & g(3) & \dots & g(1) \\ g(1) & g(n) & \dots & g(2) & 1 & 0 & \dots & 0 \\ g(2) & g(1) & \dots & g(3) & 0 & 1 & \dots & \vdots \\ \vdots & \vdots & \dots & \vdots & \vdots & \vdots & \dots & \vdots \\ g(n) & g(n-1) & \dots & g(1) & 0 & \dots & 0 & 1 \end{bmatrix} \begin{bmatrix} f_s(1) \\ f_s(2) \\ \vdots \\ f_s(n) \\ f_r(1) \\ f_r(2) \\ \vdots \\ f_r(n) \end{bmatrix} \quad (9)$$

or in shorthand notation

$$\begin{bmatrix} F_s \\ F_r \end{bmatrix} = \begin{bmatrix} I & B \\ B^T & I \end{bmatrix} \begin{bmatrix} f_s \\ f_r \end{bmatrix} \quad (10)$$

where I denotes the identity matrix (with 1's in diagonal positions and 0's elsewhere), and T denotes matrix transpose, and

$$B = \begin{bmatrix} g(1) & g(2) & \dots & g(n) \\ g(n) & g(1) & \dots & g(n-1) \\ \vdots & \vdots & \ddots & \vdots \\ g(2) & g(3) & \dots & g(1) \end{bmatrix},$$

The frequency domain Eqs. (5) and (6) become

$$\begin{bmatrix} \tilde{F}_s(k) \\ \tilde{F}_r(k) \end{bmatrix} = \begin{bmatrix} 1 & \tilde{g}(k) \\ \tilde{g}(-k) & 1 \end{bmatrix} \begin{bmatrix} \tilde{f}_s(k) \\ \tilde{f}_r(k) \end{bmatrix} \quad (11)$$

Note that here, as well as in the following, we choose n to be large enough so that both the stimulus-aligned ERP average and the response-aligned ERP average are mostly overlapped. This requires segmenting individual trials (with length n) in such a way that the periodic condition is imposed (see Zhang, 1998). See Section 5 for more details.

2.2. ERP decomposition for N components ($N > 2$)

We first consider the three-component case ($N=3$). Suppose a single-trial evoked waveform involves three different components $f_c(t)$, $f_s(t)$ and $f_r(t)$ each of which is time-locked to three different events, cue, stimulus and response, respectively. Denote the onset time as, t_c , t_s and t_r , with $t_c < t_s < t_r$. Note that fixing any one of the t 's, the others are “random” variables in the sense they vary across the trials (though some of these are controlled by the experimenter). Typically, one chooses t_c as the reference—in this case the probability distributions of $t_s - t_c$ and $t_r - t_c$, which are treated as random variables, are denoted $g_1(t)$ and $g_2(t)$, respectively. When choosing t_s as the reference, the distribution of $t_c - t_s$ and $t_r - t_s$ can be written as $g_1(-t)$ and $g_3(t)$, respectively. When choosing t_r as the reference, the distributions of t_c and t_s relative to t_r are $g_2(-t)$ and $g_3(-t)$, respectively. It is important to note that only two of the three distributions $g_1(t)$, $g_2(t)$, $g_3(t)$ are independent, for instance, $g_2(t) = g_1(t) * g_3(t)$, where $*$ denotes convolution (see discussion of Zhang, 1998, on the three component case in the context of a decision-related marker). Denote $F_c(t)$, $F_s(t)$ and $F_r(t)$ are the ensemble average ERP aligned to t_c , t_s and t_r , respectively. Then the relationship between the pure event-related components $f_c(t)$, $f_s(t)$ and $f_r(t)$ and the ensemble average signals $F_c(t)$, $F_s(t)$ and $F_r(t)$ are

$$F_c(t) = f_c(t) + f_s(t) * g_1(t) + f_r(t) * g_2(t) \quad (12)$$

$$F_s(t) = f_s(t) + f_c(t) * g_1(-t) + f_r(t) * g_3(t) \quad (13)$$

$$F_r(t) = f_r(t) + f_c(t) * g_2(-t) + f_s(t) * g_3(-t) \quad (14)$$

Following Section 2.1, the above equations can be written in matrix notation:

$$\begin{bmatrix} F_c \\ F_s \\ F_r \end{bmatrix} = \begin{bmatrix} I & A & B \\ A^T & I & C \\ B^T & C^T & I \end{bmatrix} \begin{bmatrix} f_c \\ f_s \\ f_r \end{bmatrix} \quad (15)$$

where

$$A = \begin{bmatrix} g_1(1) & g_1(2) & \cdots & g_1(n) \\ g_1(n) & g_1(1) & \cdots & g_1(n-1) \\ \vdots & \vdots & \ddots & \vdots \\ g_1(2) & g_1(3) & \cdots & g_1(1) \end{bmatrix},$$

$$B = \begin{bmatrix} g_2(1) & g_2(2) & \cdots & g_2(n) \\ g_2(n) & g_2(1) & \cdots & g_2(n-1) \\ \vdots & \vdots & \ddots & \vdots \\ g_2(2) & g_2(3) & \cdots & g_2(1) \end{bmatrix},$$

$$C = \begin{bmatrix} g_3(1) & g_3(2) & \cdots & g_3(n) \\ g_3(n) & g_3(1) & \cdots & g_3(n-1) \\ \vdots & \vdots & \ddots & \vdots \\ g_3(2) & g_3(3) & \cdots & g_3(1) \end{bmatrix}$$

Note in the above matrix-based equations in the time domain, we have imposed the periodic condition in constructing the ERP averages. As a result, $g_1(t)$, $g_2(t)$ and $g_3(t)$ are all periodic when $t > n$ or $t < 0$, so only the values of $g_i(1), \dots, g_i(n), i = 1, 2, 3$ are involved in the computation.

In frequency domain, the equations are

$$\begin{bmatrix} \tilde{F}_c(k) \\ \tilde{F}_s(k) \\ \tilde{F}_r(k) \end{bmatrix} = \begin{bmatrix} 1 & \tilde{g}_1(k) & \tilde{g}_2(k) \\ \tilde{g}_1(-k) & 1 & \tilde{g}_3(k) \\ \tilde{g}_2(-k) & \tilde{g}_3(-k) & 1 \end{bmatrix} \begin{bmatrix} \tilde{f}_c(k) \\ \tilde{f}_s(k) \\ \tilde{f}_r(k) \end{bmatrix} \quad (16)$$

This formulation from three-component can be easily extended to $N > 3$ situations. When there are N components in a single-trial ERP waveform that are time-locked to the N corresponding behavioral events that are marked by N variables $t_1, \dots, t_N, t_1 < \dots < t_N$, with $N - 1$ of them as random variables (in the sense discussed earlier). Let $f_i(t) (i = 1, \dots, N)$ denote the N component waveforms, and $F_i(t) (i = 1, \dots, N)$ denote the N ensemble averages of ERP aligned with respect to the behavioral events. Denote $g_{i,j}(t) (i = 1, \dots, N, j = 1, \dots, N, i \neq j)$ as onset time distribution of event j aligned to a fixed event i (see below). They are not all independent; only $N - 1$ of them are. We can calculate the time distribution of an arbitrary event onset time point relative to the other events onset time point. Then the following equation can be obtained

$$\begin{bmatrix} F_1 \\ F_2 \\ \vdots \\ F_N \end{bmatrix} = \begin{bmatrix} I & G_{1,2} & \cdots & G_{1,N} \\ G_{2,1} & I & \cdots & G_{2,N} \\ \vdots & \vdots & \ddots & \vdots \\ G_{N,1} & G_{N,2} & \cdots & I \end{bmatrix} \begin{bmatrix} f_1 \\ f_2 \\ \vdots \\ f_N \end{bmatrix} \quad (17)$$

where

$$G_{i,j} = \begin{bmatrix} g_{i,j}(1) & g_{i,j}(2) & \cdots & g_{i,j}(n) \\ g_{i,j}(n) & g_{i,j}(1) & \cdots & g_{i,j}(n-1) \\ \vdots & \vdots & \ddots & \vdots \\ g_{i,j}(2) & g_{i,j}(3) & \cdots & g_{i,j}(1) \end{bmatrix};$$

and $G_{i,i} = C_{j,i}^T$.

In frequency domain, the matrix-form equation is

$$\begin{bmatrix} \tilde{F}_1(k) \\ \tilde{F}_2(k) \\ \vdots \\ \tilde{F}_N(k) \end{bmatrix} = \begin{bmatrix} 1 & \tilde{G}_{1,2}(k) & \cdots & \tilde{G}_{1,N}(k) \\ \tilde{G}_{1,2}(-k) & 1 & \cdots & \tilde{G}_{2,N}(k) \\ \vdots & \vdots & \ddots & \vdots \\ \tilde{G}_{1,N}(-k) & \tilde{G}_{2,N}(-k) & \cdots & 1 \end{bmatrix} \begin{bmatrix} f_1(k) \\ f_2(k) \\ \vdots \\ f_N(k) \end{bmatrix} \quad (18)$$

3. Computer simulation: three-component decomposition

In order to test our method, we perform computer simulation on artificially generated single-trial ERP data involving three components ($N = 3$), as detailed below.

We generated 100 single trials of ERP data, with each trial made up of three different elementary “components” time-locked to three different events. The three event-related components (f_c, f_s and f_r , named for convenience as cue, stimulus and response component, respectively) are generated by Eq. (19) (Yao, 2001) so that the waveforms resemble those of evoked potential:

$$f_\beta(t_i) = \exp\left(-\left(2\pi\lambda_\beta \frac{t_i - \tau_\beta}{\gamma_\beta}\right)^2\right) \cos(2\pi\lambda_\beta(t_i - \tau_\beta) + \alpha) \quad (19)$$

$i = 1, \dots, n; \quad \beta = c, s, r,$

where $t_i = i * 0.004s = i * 4ms$ and $n = 500$. Here, the parameter values are $\gamma_c = 3.4, \gamma_s = 2.9, \gamma_r = 5.4$ and $\lambda_c = 1.5, \lambda_s = 2.0, \lambda_r = 2.7$. For each trial, $\tau_\beta (\beta = c, s, r)$ is the random variable representing onset time point for event β . Without loss of generality, we take τ_c to be fixed at 200, and $\tau_s = 250 \pm \text{Rand}$, $\tau_r = 300 \pm \text{Rand}$, where Rand represent a uniformly distributed random number with mean 0 and variance 100. The value of α is taken to be fixed between 0 and 2π . ERP waveform on any individual trial is taken to be the sum of the above three components, plus background noise as described below.

In order to simulate the background EEG, two autoregressive (AR) processes (Brockwell and Davis, 1987) and white noise are added into each trial. The coefficient of the AR2-processes is the same as used in the paper of Krieger et al. (1995). The first AR2-process mimics alpha-band activity and the second nonstationality of the background EEG. The signal-to-noise ratio is taken as 0.5.

The results of the computer simulation are shown in Fig. 1. In order to test whether the components in single trial are in accord with the decomposed waveform by our method, we apply the Wiener-filter technique of (Krieger et al., 1995) for estimating ERPs, with results shown in Fig. 2. From these figures, we conclude that our method faithfully recovers the underlying event related component for this artificially generated dataset.

4. An illustrative example

4.1. Experimental paradigm

Visual stimuli were generated by a personal computer and displayed on a monitor with dark background. Subjects were being seated 50 cm in front of the monitor and instructed to fixate on a center cross extending 0.5° visual angle (the fixation point). Two rectangular boxes, each of size $1.5^\circ \times 1.0^\circ$, were horizontally located at 5° visual angle on either side from the fixation point. As a trial starts, two boxes located in the left and right of the fixation cross appeared for a duration of 120 ms, then one of the boxes was brightened (thickened) for 50 ms, serving as a “cue” for the location of the stimulus to appear later. Then, following a random delay between 100 ms and 300 ms after the disappearance of the thickened perimeter of the box, a stimulus was presented for 200 ms. The stimulus can be either a short vertical line (0.75° visual angle) or

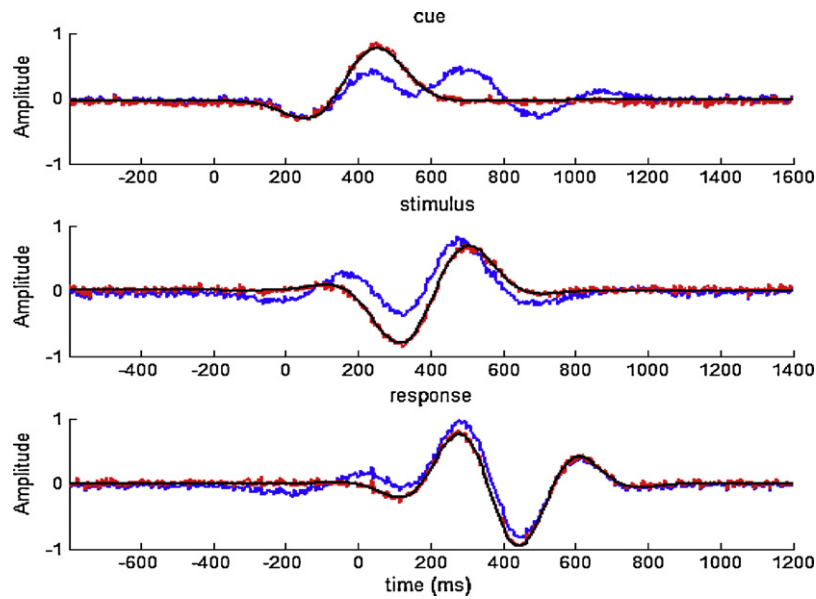


Fig. 1. Demonstration of recovery of artificial data with three components decomposition. Each panel plots the artificially generated ERP component (black), the recovered component (red), and the event-aligned ERP average (blue). The top, middle, bottom panels display the three waveforms mentioned above when time-locked ($t=0$) to cue onset, stimulus onset, response onset, respectively. Red curves: recovered cue/stimulus/response-locked components; blue curves: original artificially generated cue/stimulus/response-aligned average ERPs; black curves: true underlying cue/stimulus/response components. (For interpretation of the references to color in this figure legend, the reader is referred to the web version of the article.)

a long vertical line (1.0° visual angle), the stimulus was presented within either box with equal probability following cue presentation, leaving the cue “valid” on half of the trials and “invalid” on the other half. Subjects were instructed to respond to the short vertical line (“target”) as quickly as possible—they were to press the key “1” with their left-hand when the short line appeared in left visual field and press key “4” with their right-hand when the short line appear on the right visual field, and refrain from responding to the long vertical line (“non-target”). All subjects performed 10 experimental blocks, with 80 trials in each block. There is a

1000–1200-ms inter-trial interval (ISI) from the subject’s response and the start of the next trial. The experimental paradigm is shown in Fig. 3.

EEG was recorded with the 128-channel EGI system at a sampling rate of 250 Hz, and vertex (Cz) was taken as the reference. Epochs contaminated with excessive eye movements, blinks, muscle artifacts, or amplifier blocking were manually removed prior to averaging, and recordings of seven in eight subjects were valid for further processing. The ERP were re-referenced to the average reference during off-line data processing.

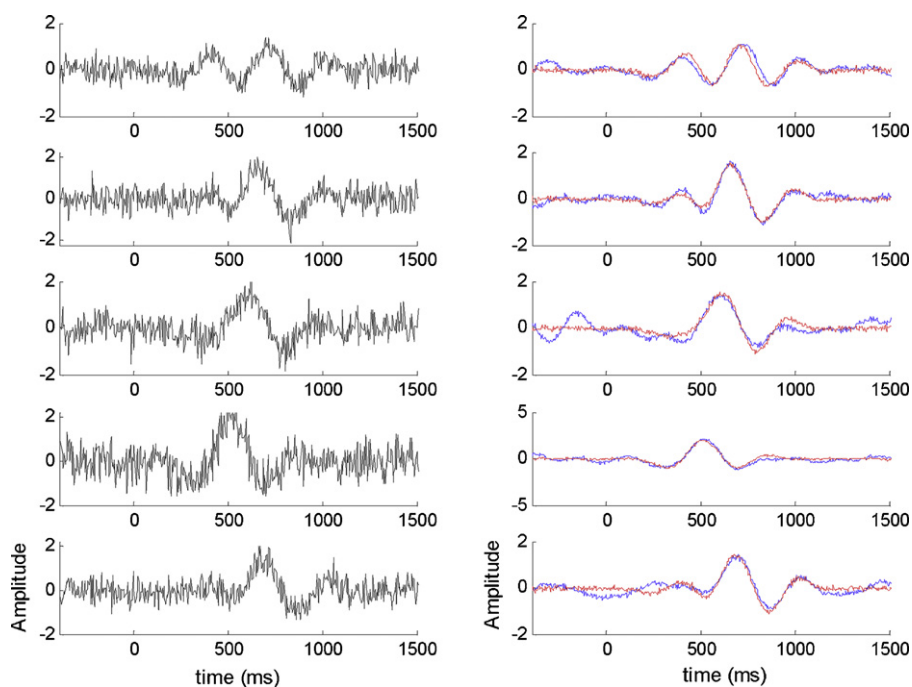


Fig. 2. Comparison of Wiener-filter method and our method on artificially generated single trial data. Left: five single trials randomly selected from 100 trials as described in the section on Computer Simulation. Here 0 is cue onset time point. Right: estimated based on Wiener-filter (blue curve) and recovered based on our method (red curve).

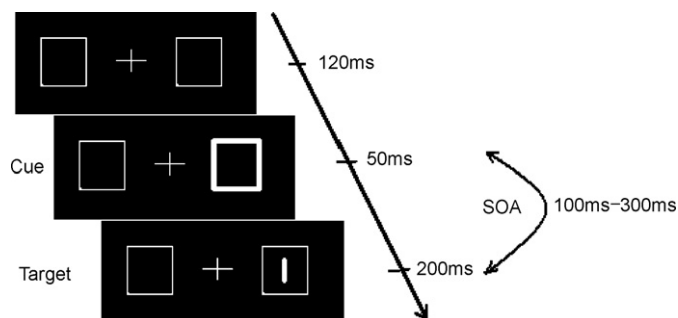


Fig. 3. An example of the stimulus display sequences used in this experiment. The cue is a brightening/thickening of one of the square boxes on either side of the fixation cross. The target is a short vertical line inside the box. Interval between cue and stimulus (SOA) varies randomly from trial to trial between 100 and 300 ms.

Eight normal male subjects (mean age 25 years, range 23–31 years) participated in this study. All were right-handed, and none had a previous history of any neurological or psychiatric disorder. Due to inadvertent recording error that occurred for one subject, only seven subjects finished this experiment and their data were analyzed.

In this paper, data from two experimental conditions were analyzed, one when the cue is valid (cue is on the left, the target short-line is also on the left, and the response is a left key-press, referred to as “cue-valid condition”) and the other when the cue is invalid (cue is on the right, the target short-line is on the left, and the response is a left key-press, referred to as “cue-invalid condition”). Both conditions have the same target location (left) and the same behavioral response.

4.2. Operation of the decomposition algorithm

To demonstrate the result of our decomposition algorithm, we use data of all the correct trials from one subject—the cue is located in the left, the stimulus is a short vertical line (“target”) located in left, and the subject responded correctly by a left-hand key-press (cue-valid condition). ERP data was taken at electrode Pz with a total of 127 trials under analysis. As described in Section 2, the cue-aligned, stimulus-aligned and response-aligned ERP averages (denoted F_c , F_s and F_r) were constructed by aligning the waveforms on individual trials with respect to cue-, stimulus- and response-onset respectively and summing over those waveforms bin-by-bin (each bin is 1 ms). The event time (cue, stimulus, response) distributions were simply constructed from these 127 trials whose durations are available around cue-onset, stimulus-onset and response-onset, respectively. The evoked component waveform related (i.e., time-locked) to cue, stimulus, and response, respectively, are denoted f_c , f_s and f_r . They are recovered by the numerical algorithm based on Eq. (16). Fig. 4 demonstrates the result of this decomposition.

Note that in the calculation of convolution operation, truncation of the convolution kernel will introduce distortion. So we adopted a temporal window (value of n) large enough to cover the entire region of interest, i.e. extending to a time-mark considerably before the first event onset and considerably after the last event onset. We also applied periodic condition in constructing the event-aligned ERP averages.

It should also be pointed out that the event related component waveforms are recoverable only in the sense that the trial-by-trial waveform is a superposition of the component waveforms separated by the event time distributions; when the event-aligned ensemble average is constructed, the resultant ERPs will be as given by the experimental data. Though theoretically the component waveforms are always uniquely recoverable from the event-aligned

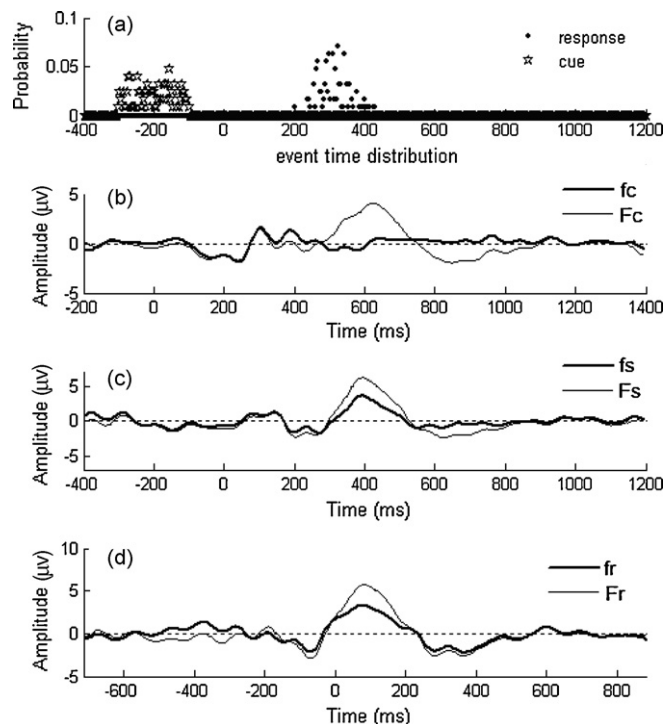


Fig. 4. Recovery of cue-, stimulus- and response-locked component waveforms at electrode Pz, denoted as f_c , f_s and f_r , respectively, the cue-, stimulus- and response-aligned ERP average denoted as F_c , F_s and F_r respectively. (a) Event time distribution is given with respect to stimulus onset, where stimulus onset time is at 0 ms. (b) Recovered cue-locked component waveform and cue-aligned ERP waveform, with cue onset time labeled as 0 ms. (c) Recovered stimulus-locked component waveform and stimulus-aligned ERP waveform, with stimulus onset time labeled as 0 ms. (d) Recovered response-locked component waveform and response-aligned ERP waveform, with response onset time as 0 ms.

ensemble averages, the result will be influenced by the signal-to-noise level as well as whether enough trials are collected to yield larger event-time distributions variance. See discussions in Zhang (1998).

4.3. Results

We applied the above-described method to decompose the cue-, stimulus-, and response-locked component waveforms in the ensemble averaged ERP (averaged across all seven subjects) as well as to the ERP averages of individual subjects. ERP data were from electrode Pz.

Fig. 5 shows the result of this decomposition of the cue-, stimulus-, and response-locked component waveforms for, respectively, the cue-valid and cue-invalid conditions from an analysis of ERP ensemble (grand) averages across seven subjects, under different alignment (reflected in top, middle, and bottom panels of these two figures) across individual trials. The top panels (of Fig. 5) show that the reconstructed cue-locked component waveform f_c is consistent with the cue-aligned ERP average F_c during the first 300 ms after cue onset, but mostly tends to flatten 500–1100 ms after cue-onset; this is contrasted with the amplitude of the cue-aligned ERP average F_c , which is still largely non-zero during this period. This is a reasonable finding, since we expect cue processing to have been completed by 500 ms when the brain will shift towards the processing of the stimulus and then of the response. The large, non-zero amplitude in F_c between the time segment 500–1100 ms reflects a cross-contamination from the stimulus-related and response-related neural processes that have not been “averaged out” in cue-aligned averaging. The middle panels of

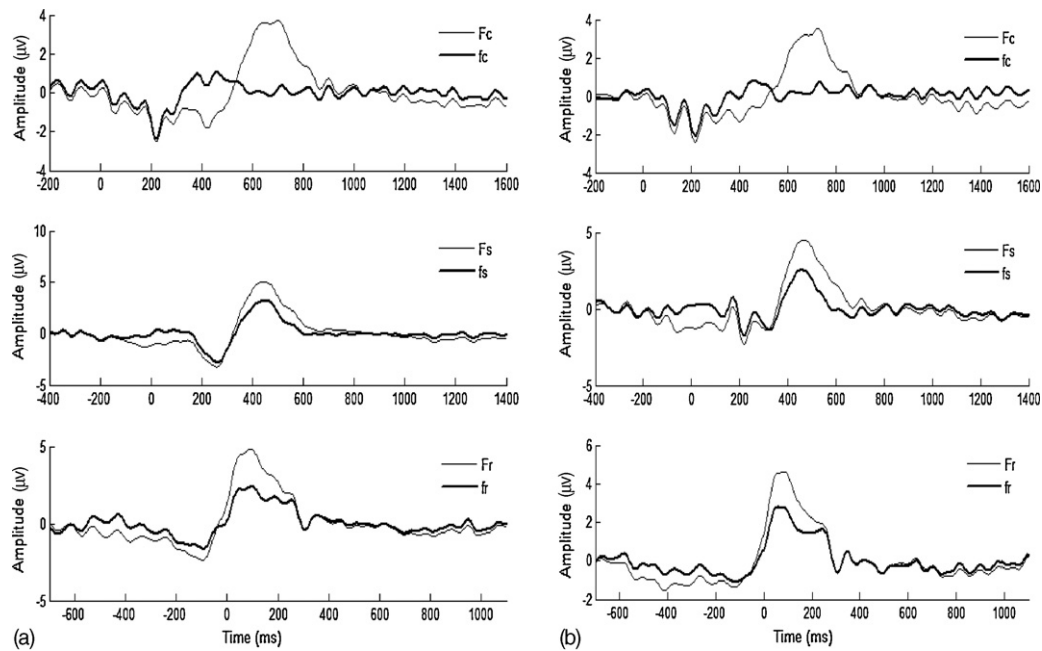


Fig. 5. Recovered cue-locked (top panel), stimulus-locked (middle panel), and response-locked (bottom panel) component waveforms (f_c , f_s and f_r) from ERP ensemble averages (aligned to cue, stimulus, and response (F_c , F_s and F_r), respectively for top, middle, and bottom panels) across all seven subjects. Thick lines: recovered cue-, stimulus-, response-locked component waveforms, and thin lines: cue-, stimulus-, response-aligned ERP ensemble averaged (across all seven subjects). (a) Cue-valid condition and (b) cue-invalid condition.

Fig. 5 plot the stimulus-aligned ERP average F_s and the recovered stimulus-locked component waveform f_s . They mainly differ in the range of 300–800 ms after stimulus onset, where the amplitude of f_s is much smaller than F_s , since the latter contains cross-contamination from the response-locked component. Similarly, the bottom panels of Fig. 5 plot the response-aligned ERP average F_r and the response-locked component f_r , where F_r is obviously larger in amplitude than that of f_r in the period 0–200 ms after behavioral onset. This, again, is presumably due to the cross-contamination of stimulus-locked component in F_r .

Figs. 6 and 7 display the recorded cue/stimulus/response-aligned ERP averages and the recovered cue/stimulus/response-locked component waveforms for all seven individual subjects. The three columns show cue-, stimulus-, and response-referenced ERP averages and component waveforms. Fig. 6 is for the cue-valid condition and Fig. 7 is for the cue-invalid condition, respectively. The reconstructed cue-locked, stimulus-locked and response-locked component waveforms are all different from the cue-aligned, stimulus-aligned and response-aligned ERP waveforms, respectively, due to the cross-contamination when stimulus-onset and response-onset vary randomly across trials. This difference is more pronounced between cue-aligned waveform and cue-locked average across all subjects.

Next, we compare the cue-valid and cue-invalid experimental conditions in Fig. 8 by plotting the recovered cue-locked component waveforms (top panel), the recovered stimulus-locked component waveforms (middle panel), and the recovered response-locked component waveforms (bottom panel) in the two conditions. In order to compare the recovered cue-locked, stimulus-locked, and response-locked component waveforms across the cue-valid and cue-invalid conditions, we compared the mean amplitude of the two waveforms during the periods of 100–300 ms after cue onset, 100–300 ms after stimulus onset, 300–500 ms after stimulus onset, and 0–200 ms after response onset, and applied t -test to the dataset of seven subjects (see Table 1, Part A). We also compared the waveform of the two conditions directly, by calculating the L_2 norm (Euclidian distance) between the two waveforms for the two condi-

tions (see Table 1, Part B). It is clear that the cue-locked waveforms are virtually identical for the cue-valid and the cue-invalid conditions, since before stimulus onset, the meaning of the cue in terms of its validity is identical and undifferentiated. At the other end, the response-locked component waveforms are also identical across the two conditions of cue-validity, indicating that the response processing stage is engaged in the same fashion independent of the status of the cue. The only stage that a valid cue and an invalid cue differ is with respect to the processing of the stimulus, where the two waveforms differ significantly (middle panel). This supports the idea that the presence of a cue affects stimulus processing due to priming on the location that a stimulus might appear.

5. Discussions

Traditionally, methods for decomposition of multiple components in ERP/EEG and fMRI data include Independent Component Analysis ICA (Bell and Sejnowski, 1995, 1997; Comon, 1994; Jutten and Herault, 1991) and Principal Component Analysis, PCA (Jackson, 1991; Jolliffe, 1986). PCA is a now-standard technique in statistical data analysis, feature extraction, and data reduction, aiming at decomposing observed signals into a linear combination of orthogonal principal components, while ICA is a technique of array processing and data analysis, aiming at recovering unobserved signals or “sources” from observed mixtures, based on the assumption of mutual independence between the underlying components. Although PCA and ICA have been widely applied in ERP/EEG and fMRI dataset analysis for artifact removal, source imaging, and feature extraction (Makeig et al., 1999; Bugli and Lambert, 2007; Makeig et al., 1996; Makeig et al., 1997; Kayser and Tenke, 2006; Niazy et al., 2005; Laeven et al., 2001), these two methods made strong assumptions which may constrain their application. For example, ICA assumes that the underlying sources are statistically independent, whereas for PCA, the underlying components are assumed to be orthogonal to one another. For one thing, independence and orthogonality may be too strong assumptions to be neurobiologically realistic (Mitr and Pesaran,

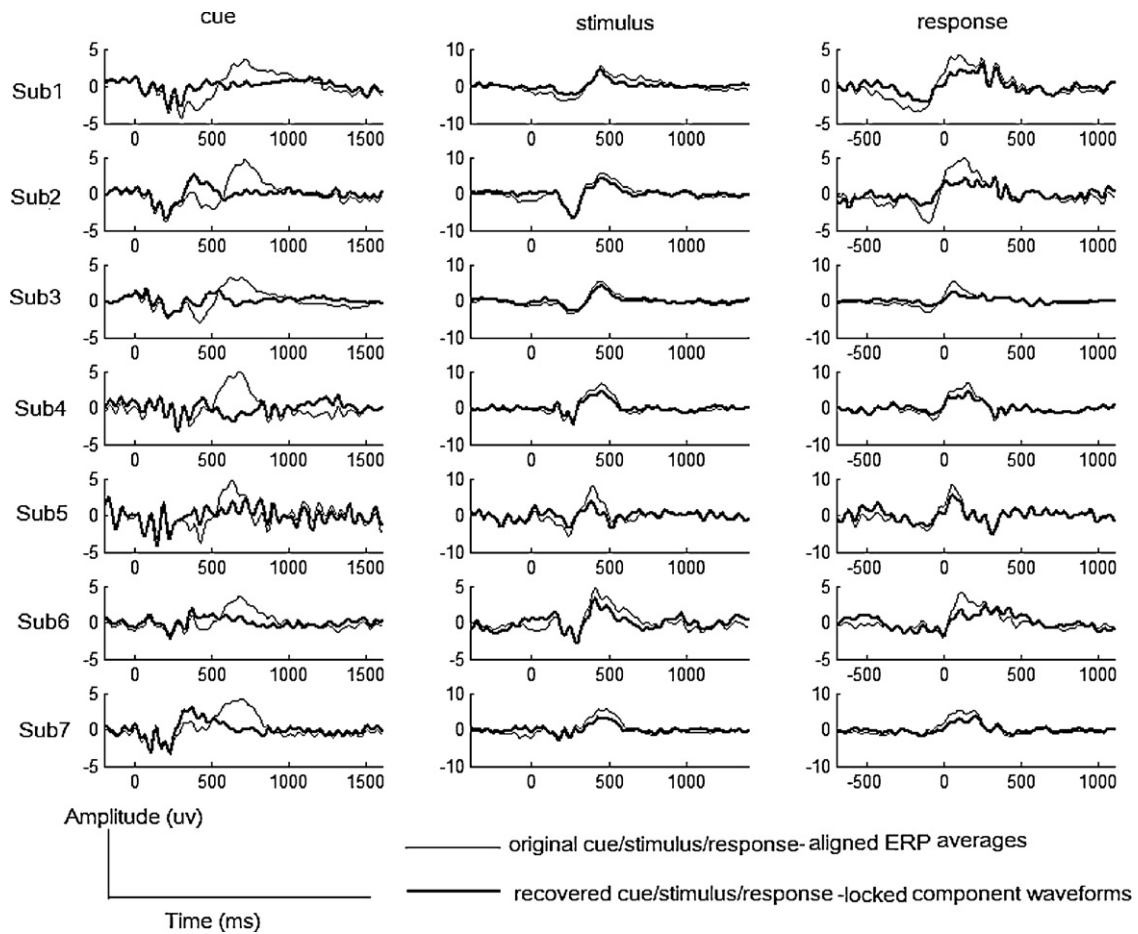


Fig. 6. The recovery result for each individual subjects at electrode Pz for the cue-valid. Thin curves are cue/stimulus/response-aligned ERP averages, and thick curves are recovered cue/stimulus/response-locked component waveforms.

1999). For both methods, the exact number of recovered components is often determined in an ad hoc fashion, by comparing the amount of variance captured versus the residual variance; the maximal number of recovered components is further constrained by the total number of observed channels for ICA and PCA. However, from a methodological point of view, both methods assume each trial is a stationary point process; therefore, they are not immediately applicable to situations where individual trials vary in their duration in terms of some key behavioral events (such as reaction time, the time between stimulus onset and behavioral response onset). The trial-by-trial variation of behavioral markers causes problem even to align EEG/fMRI recordings on

these trials properly, which is a precursor for ICA/PCA type analysis.

This last constraint is crucial for successful methods of decomposing EEG/fMRI components for many psychological experiments which, typically, involve two or more behavioral events in a single trial. This problem is, fortunately, completely solved for $N=2$ components (Zhang, 1998). There, stimulus-aligned and response-aligned ERP averages are being used (along with the reaction-time distribution) to uniquely recover a stimulus-locked and response-locked component.

Here, this method is extended to $N>2$; we developed a multi-component ERP decomposition algorithm for isolating ERP

Table 1

Results of comparing the cue-valid) and cue-invalid experimental conditions. Part A presents the result of statistical tests. Part B shows L2-norm of recovered waveforms of the two experimental conditions.

Recovered component	Cue-valid (mean amplitude)	Cue-invalid (mean amplitude)	p-Value
A			
f_c (100–300 ms)	–1.015 μ V	–1.026 μ V	0.9769 > 0.05
f_s (100–300 ms)	–1.2556 μ V	–0.4564 μ V	0.0365 < 0.05
f_s (300–500 ms)	1.8049 μ V	0.8859 μ V	0.0059 < 0.05
f_r (0–200 ms)	1.7932 μ V	1.9545 μ V	0.7207 > 0.05
Component			L2 norm (Euclidian distance)
B			
f_c (cue-valid) vs. f_c (cue-invalid)			7.25
f_s (cue-valid) vs. f_s (cue-invalid)			11.26
f_r (cue-valid) vs. f_r (cue-invalid)			6.22

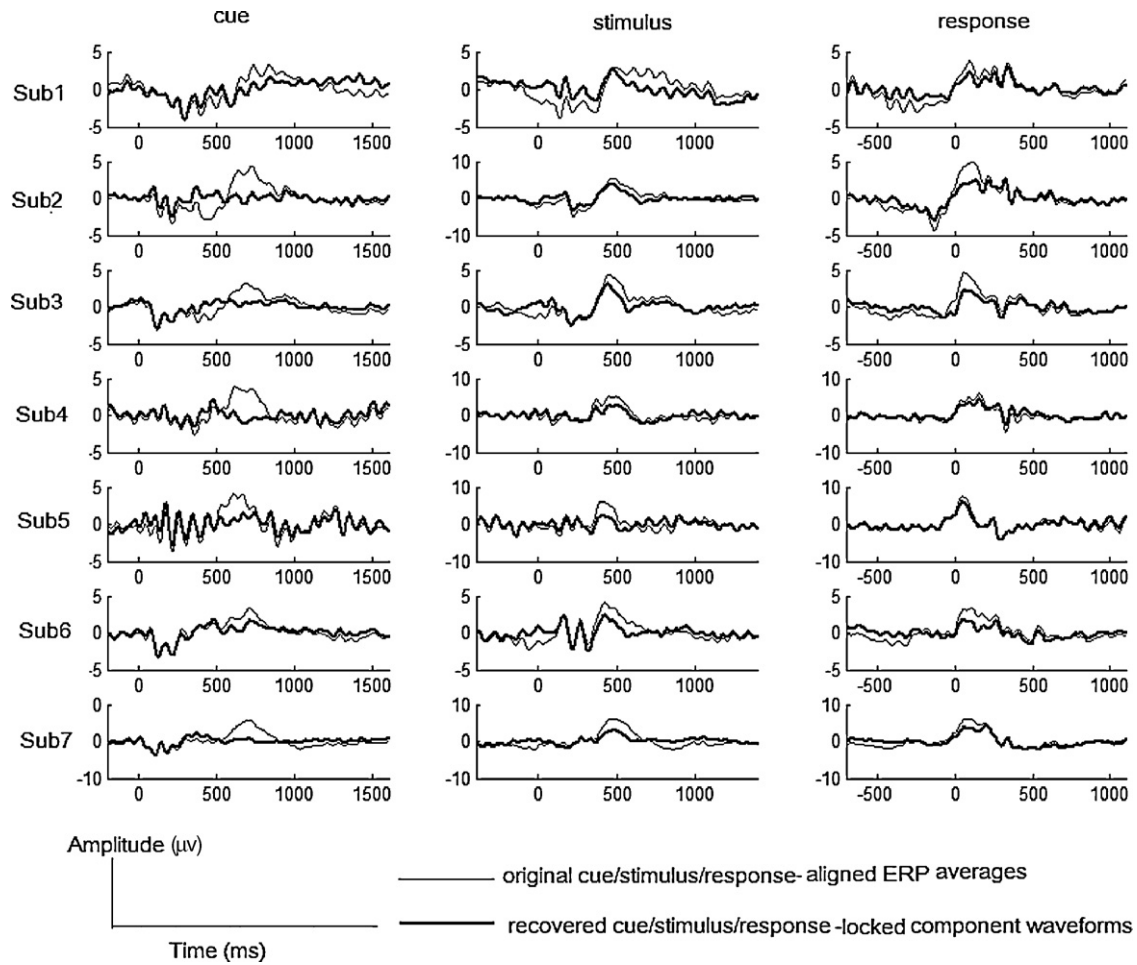


Fig. 7. Same as Fig. 6, except that the experimental condition is cue-invalid.

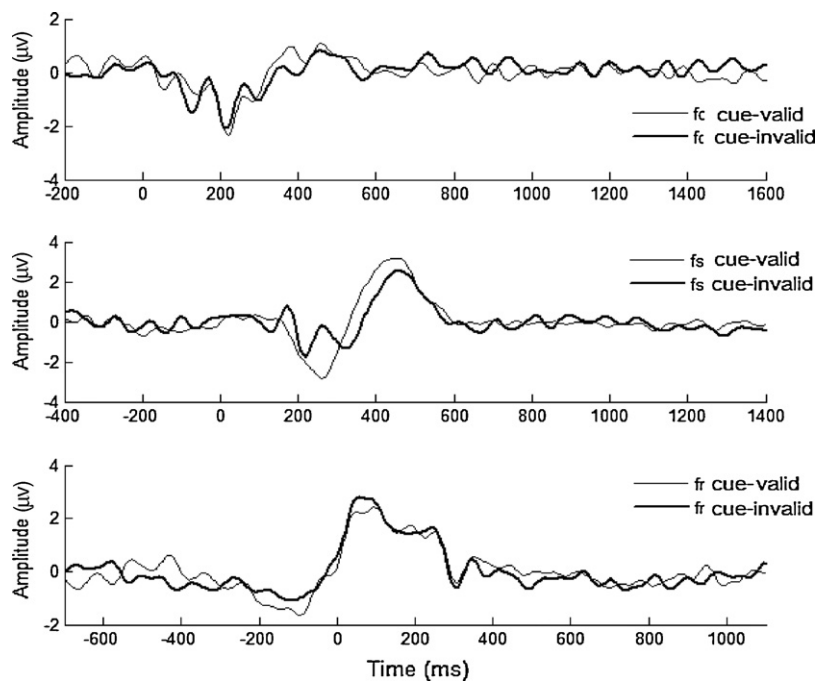


Fig. 8. Comparison of the average recovered cue-locked, stimulus-locked, and response-locked component waveforms of all seven subjects across the cue-valid and cue-invalid conditions.

component waveforms time-locked to *N*-specific behavioral events during a trial. In contrast to such methods as PCA/ICA, our multi-component decomposition algorithm solves the non-stationarity problem of time series (i.e., ERP/fMRI recordings across trials) where trial-by-trial variation in the passage of time is of behavioral significance.

Our simulation results demonstrate that our method is effective and practicable in disentangling the contribution of different components time-locked to various behavioral events. However, we also note that the effectiveness of the method relies heavily on the “proper” shape of event time distribution across the ensemble of trials. Here “proper” means that the variance of distribution is significantly different from zero. Actually, the less variance the event time distribution has, the less effective the method becomes. Mathematically, when the event variance is small (i.e., all trials have nearly uniform reaction time), its Fourier transform approaches unity and the recovery error generated by applying Eq. (16) or (18) becomes large. At the other extreme, when say the reaction time distribution has too large a variance that exceeds the *average* reaction time, the event-aligned ERP waveforms will have included late or early contributions outside the region of interest. Technically, to get the event-aligned ERPs across individual trials, we need to segment the raw EEG recording into single trials all with same length and then impose periodic condition in order to perform the Fourier transform (see Section 2)—the variance of event distribution need to be small enough so that the segmented single trial recording still contains the region of interest.

Notwithstanding such technical constraints, our method actually addresses and solves a problem when other traditional methods may fail (i.e., when event time distributions are large), so it is a completely complementary technique in ERP multi-component analysis. Though our simulations are based on ERP context, the basic mathematical technique behind our method can also be easily adapted to deal with event-related signals in other neuro-imaging studies (e.g. fMRI), such that trial-by-trial variation in behavioral reaction time is no longer an obstacle but rather an opportunity for isolating the underlying neurocognitive processes mediating a task.

Acknowledgements

The work was supported by the 973 project 2003CB716106, Chinese NSF grants NSFC #30525030 and #60736029 awarded to the University of Electronic Science and Technology of China, and by AFOSR research grant FA9550-06-0298 awarded to the University of Michigan. Gang Yin is also partially supported by a fellowship from China Scholarship Council.

References

- Bell AJ, Sejnowski TJ. The 'Independent Components' of natural scenes are edge filters. *Vision Research* 1997;37(23):3327–38.
- Bell AJ, Sejnowski TJ. An information maximization approach to blind separation and blind deconvolution. *Neural Computation* 1995;7(6):1129–59.
- Brockwell P, Davis R. *Time series: theory and methods*. New York: Springer; 1987.
- Bugli C, Lambert P. Comparison between principal component analysis and independent component analysis in electroencephalograms modeling. *Biometrical Journal* 2007;49(2):312–27.
- Comon P. Independent component analysis—a new concept. *Signal Processing* 1994;36:287–314.
- Falkenstein M, Koshlykova NA, Kiroi VN, Hoormann J, Hohnsbein J. Late ERP components in visual and auditory Go/Nogo tasks. *Electroencephalography and Clinical Neurophysiology* 1995;96:36–43.
- Gehring WJ, Fencsik D. Slamming on the breaks: an electrophysiological study of error response inhibition. In: Poster presented to the annual meeting of the cognitive neuroscience society; 1999. p. 11–3.
- Gehring WJ, Goss B, Coles MG, Meyer DE, Dochin E. A neural system for error detection and compensation. *Psychological Science* 1993;4:385–90.
- Hillyard SA, Picton TW. *Electrophysiology of cognition*. In: Plum E, editor. *Handbook of physiology: the nervous system*, vol. V. Bethesda, MD: American Physiological Society; 1987. p. 519–84.
- Jackson JA. *A users guide to principal component analysis*. New York: Wiley; 1991.
- Jolliffe IT. *Principal component analysis*. New York: Springer-Verlag; 1986.
- Jutten C, Herault J. Blind separation of sources. Part I. An adaptive algorithm based on neuromimetic architecture. *Signal Processing* 1991;24:1–10.
- Kayser J, Tenke CE. Principal components analysis of Laplacian waveforms as a generic method for identifying ERP generator patterns. I. Evaluation with auditory oddball tasks. *Clinical Neurophysiology* 2006;17(2):348–68.
- Krieger S, Timmer J, Lis S, Olbrich HM. Some considerations on estimating event-related brain signals. *Journal of Neural Transmission [Gen Sect]* 1995;99:103–29.
- Kok A. Effects of degradation of visual stimulation on components of the event-related potential (ERP) in go/nogo reaction tasks. *Biological Psychology* 1986;23:21–38.
- Kopp B, Mattler U, Goertz R, Rist F. N2, P3 and the lateralized readiness potential in a nogo task involving selective response priming. *Electroencephalography and Clinical Neurophysiology* 1996;99:19–27.
- Kutas M, Hillyard SA. Event-related brain potentials to semantically inappropriate and surprisingly large words. *Biological Psychology* 1980;11:99–116.
- Laeven R, Gielen CCAM, Coenen AML, Van Rijn CM. Principal Component Analysis and Gabortransform in analysing burst-suppression EEG under propofol anaesthesia. *Sleep-Wake Research in the Netherlands* 2001;12:75–80.
- Makeig S, Bell AJ, Jung T-P, Sejnowski TJ. Independent component analysis of electroencephalographic data. *Advances in Neural Information Processing Systems* 1996;8:145–51.
- Makeig S, Jung T-P, Bell AJ, Sejnowski TJ. Blind separation of auditory event-related brain responses into independent components. *Proceedings of National Academy of Sciences* 1997;94:10979–84.
- Makeig S, Westerfield M, Jung T-P, Covington J, Townsend J, Sejnowski TJ, et al. Functionally independent components of the late positive event-related potential during visual spatial attention. *The Journal of Neuroscience* 1999;19(April (7)):2665–80.
- Mitr PP, Pesaran B. Analysis of dynamic brain imaging data. *Biophysics Journal* 1999;76:691–708.
- Niazy RK, Beckmann CF, Iannetti GD, Brady JM, Smith SM. Removal of fMRI environment artifacts from EEG data using optimal basis sets. *Neuroimage* 2005;28:720–37.
- Simson R, Vaughan HG, Ritter W. The scalp topography of potentials in auditory and visual go/nogo tasks. *Electroencephalography and Clinical Neurophysiology* 1977;43:864–75.
- Squires NK, Squires KC, Hillyard SA. Two varieties of long-latency positive waves evoked by unpredictable auditory stimuli in man. *Electroencephalography and Clinical Neurophysiology* 1975;38:387–401.
- Yao D. A method to standardize a reference of scalp EEG recording to a point at infinity. *Physiological Measurement* 2001;22:693–711.
- Zhang J. Decomposing stimulus and response component waveforms in ERP. *Journal of Neuroscience Methods* 1998;80:49–63.